Published in final edited form as:
Dev Cell. 2013 April 15; 25(1): 93–105. doi:10.1016/j.devcel.2013.02.016.

Regional modulation of a stochastically expressed factor determines photoreceptor subtypes in the *Drosophila* retina

Shivani U. Thanawala[1], **Jens Rister**[1], **Gregory W. Goldberg**[1,2], **Andrey Zuskov**[1], **Eugenia C. Olesnicky**[3,4], **Jonathan M. Flowers**[5,6], **David Jukam**[1], **Michael D. Purugganan**[5,6], **Elizabeth R. Gavis**[3], **Claude Desplan**[1,6], and **Robert J Johnston Jr.**[1,*]

[1]Center for Developmental Genetics, Department of Biology, New York University, New York, NY 10003, USA

[3]Department of Molecular Biology, Princeton University, Princeton, NJ 08544, USA

[4]Department of Biology, University of Colorado at Colorado Springs, Colorado Springs, CO 80918, USA

[5]Center for Genomics and Systems Biology, Department of Biology, New York University, New York, NY 10003 USA

[6]Center for Genomics and Systems Biology, NYUAD Institute, New York University, Abu Dhabi, United Arab Emirates

Abstract

Stochastic mechanisms are sometimes utilized to diversify cell fates, especially in nervous systems. In the *Drosophila* retina, stochastic expression of the PAS-bHLH transcription factor Spineless (Ss) controls photoreceptor subtype choice. In one randomly distributed subset of R7 photoreceptors, Ss activates Rhodopsin4 (Rh4) and represses Rhodopsin3 (Rh3); counterparts lacking Ss express Rh3 and repress Rh4. In the dorsal third region of the retina, the Iroquois Complex transcription factors induce Rh3 in Rh4-expressing R7s. Here, we show that Ss levels are controlled in a binary On/Off manner throughout the retina, yet are attenuated in the dorsal third region to allow Rh3 co-expression with Rh4. Whereas the sensitivity of *rh3* repression to differences in Ss levels generates stochastic and regionalized patterns, the robustness of *rh4* activation ensures its stochastic expression throughout the retina. Our findings show how stochastic and regional inputs are integrated to control photoreceptor subtype specification in the *Drosophila* retina.

Introduction

The *Drosophila* eye provides an excellent paradigm to study how stochastic and regionalized regulatory inputs intersect to affect cell fate specification. Underlying its uniform morphology, the fly eye contains two randomly distributed subtypes of ommatidia (unit eyes) defined by the mutually exclusive expression of specific Rhodopsin (Rh) proteins in the inner photoreceptors (R7 and R8). In the pale (**p**) subtype, **p**R7s express Rhodopsin3

*Corresponding author: rjj210@nyu.edu.
[2]Current Address: Laboratory of Bacteriology, The Rockefeller University, New York, NY 10065, USA

(Rh3) and **p**R8s express Rhodopsin5 (Rh5), whereas in the yellow (**y**) subtype, **y**R7s express Rhodopsin4 (Rh4) and **y**R8s express Rhodopsin6 (Rh6). Though the **p** and **y** subtypes are randomly distributed, they consistently occur in a **p:y** ratio of approximately 35:65 (Bell et al., 2007; Johnston Jr and Desplan, 2010) (Figure 1A–B, 1D, 1F). Throughout the majority of the retina, the mutually exclusive expression of Rhs defines the **p** and **y** ommatidial subtypes. However, in the dorsal third region of the retina, Rh3 is co-expressed with Rh4 in **y**R7s. Thus, the dorsal third region consists of **p** ommatidia containing **p**R7s that express Rh3 only and "dorsal third **y**" ommatidia containing **y**R7s that express both Rh4 and Rh3 (Figure 1C–E) (Mazzoni et al., 2008).

Stochastic ommatidial subtype specification is controlled by the PAS-bHLH transcription factor Spineless (Ss) (Wernet et al., 2006). Ss is expressed in a random subset of R7s where it determines **y** subtype fate. In **y**R7s, Ss has three main functions: (1) activate Rh4, (2) repress Rh3, and (3) repress a signal from R7 to R8, leading to the default **y**R8 fate (Rh6 expression) (Figure 1B). In the absence of Ss, **p**R7 fate (Rh3 expression) and **p**R8 fate (Rh5 expression) are induced (Figure 1 A).

yR7-specific expression of Rh4 appears to be simply activated by Ss. In contrast, **p**R7-specific expression of Rh3 is regulated by complex interlocked feedforward loops of transcription factors (Johnston et al., 2011). The Defective Proventriculus (Dve) homeodomain protein, a repressor that directly binds the *rh3* promoter, is a critical node in this motif (Figure 1A–B). The Orthodenticle (Otd) homeodomain protein activates Dve expression in all PRs, whereas the Spalt zinc finger transcription factors (Salm and Salr, referred to collectively as "Sal") repress Dve in R7s (Figure 1A–B). In **p**R7s, Sal and Otd together activate Rh3 in the absence of Dve (Figure 1A). In **y**R7s, Ss re-activates Dve which represses Rh3 despite the presence of Otd and Sal (Figure 1B) (Johnston et al., 2011; Sood et al.,2012).

The regionalized co-expression of Rh3 in Rh4-expressing yR7s in the dorsal third of the retina is activated by the transcription factors of the Iroquois Complex (IroC) Figure 1C–E) (Mazzoni et al., 2008). Whereas Ss provides a stochastic input, IroC supplies a regionalized input into the regulation of Rh expression.

Here, we show that, as in other biological contexts, Spineless acts with the ubiquitously expressed PAS-bHLH protein, Tango (Tgo) (Emmons et al., 1999), to regulate Rh expression. We show that the proper stochastic and regional control of Rh expression requires five mechanistic features: (1) Ss levels are high in **y**R7s in the main part of the retina to ensure repression of Rh3 and activation of Rh4, (2) Ss levels are reduced in dorsal third **y**R7s to allow Rh3 expression, (3) IroC activates Rh3 in dorsal third **y**R7s, (4) low Ss levels (as found in dorsal third **y**R7s) are sufficient to activate Rh4 expression, and (5) the absence of Ss expression produces **p**R7 fate including expression of Rh3 and absence of Rh4. The sensitivity of *rh3* to regional inputs is likely due to the presence of multiple IroC (activating) and Dve (repressing) binding sites in the *rh3* promoter, whereas the robustness of Rh4 activation appears to be due to the presence of a single Ss (activating) binding site. Our data demonstrate how stochastic and regionalized regulatory inputs are integrated to determine ommatidial subtype specification throughout the retina.

Results

Tgo is required for stochastic Rh expression

In most biological contexts, the Tgo PAS-bHLH transcription factor is required as a heterodimeric partner for Ss function. Ss is expressed in specific cell types where it binds ubiquitously-expressed Tgo in the cytoplasm. The Ss/Tgo heterodimer then localizes to the

nucleus to regulate target genes (Emmons et al., 1999; Ward et al., 1998). Although it has been suggested that Ss works independently of Tgo in some contexts, these analyses were conducted with available *tgo* alleles, which were all hypomorphs (Kim et al., 2006).

Because we could not detect staining in the eye using the available Tgo antibody (data not shown), we generated a *tgo* transcriptional reporter (*tgo^{prom}>nuGFP*) that drove GFP expression in all cells in the retina including all R7 cells, consistent with previous reports that Tgo is ubiquitously expressed (Figure 2o).

To clearly ascertain the role of Tgo in stochastic Rh regulation, we generated two *tgo* null mutant alleles, *tgo^{del6}* and *tgo^{del25}*, using the hobo transposable element system (see Materials and Methods). *tgo^{del6}* removes the bHLH, PAS, and PAC domains required for dimerization and DNA binding, whereas *tgo^{del25}* removes the entire *tgo* locus and part of the 3' UTR region of the neighboring *cg11986* gene (Figure 2A–B). Both *tgo^{del6}* and *tgo^{del25}* null mutant retinas displayed expression of Rh3 and loss of Rh4 in all R7s, similar to ss mutants (Figure 2D–E, Figure S1A). Retinas in which *tgo* was knocked down using RNAi as well as *tgo* null mutant clones displayed a similar phenotype (Figure 2F, 2J, S1B). *tgo* null mutants faithfully phenocopied ss null mutants for all features of Rh regulation including de-repression of the signal to R8s causing a dramatic increase in the frequency of Rh5-expressing R8s (Figure 2H–I), loss of Dve expression in **y**R7s (Figure 2L), and no effect on general cell fate markers (Figure S1C–G)

Consistent with the requirement of Ss/Tgo dimerization for efficient localization to the nucleus, Ss was not detectable in nuclei in *tgo* null mutant clones (Figure 2K). Further, although we could detect nuclear Ss in all photoreceptors when provided ectopically by a strong heterologous promoter (*IGMR>Gal4*), this localization was dramatically weaker in *tgo* mutant tissue compared to neighboring wild type tissue (Figure 2N).

Tgo is cell-autonomously required for regulation of Rh expression by Ss since ectopically-expressed Ss induced expression of Rh4 in all PRs and repression of Rh3 in all R7s in wild type clones, but failed to do so in *tgo* null mutant clones, leading to Rh3 expression and loss of Rh4 in all R7s (Figure 2M).

Ss is also required for the elaboration of dendrites in 'dendrite arborization' (da) sensory neurons. Although the hypomorphic *tgo^{5}* allele exhibited no dendritic arborization defects (Kim et al., 2006), *tgo* null mutant clones displayed decreases in the number of dendritic termini similar to ss null mutants, suggesting that Tgo is required for all Ss functions (Figure S1H–L).

Stochastic binary On/Off regulation and regional modulation of levels determines Ss expression

Rh3 and Rh4 are expressed in mutually exclusive R7 subtypes in the main part of the retina. However, in the dorsal third region, IroC activates Rh3 co-expression in Rh4-expressing yR7s. We hypothesized that Ss could also play a role in this co-expression phenomenon and thus, we assessed the levels of Ss protein to determine regional differences across the retina. We defined four regions of the retina based on ommatidium position relative to the equator: dorsal third (DT), dorsal equatorial (DE), ventral equatorial (VE), and ventral third (VT). Ss was expressed in an On/Off manner across the retina as indicated by the bimodal distributions for each region (Figure 3A–H). Interestingly, Ss levels were significantly lower for cells in the On state in the DT than in other regions of the eye (Figure 3A–B). Ss levels in *IroC* mutant clones were comparable to neighboring wild type tissue (Figure 3I–J) and ectopic expression of IroC in all R7s did not significantly reduce Ss levels (data not shown), showing that this reduction of Ss levels in the DT is IroC-independent.

Rh3 and Rh4 are differentially responsive to Ss/Tgo activity levels

We hypothesized that the reduced levels of Ss in the DT lower repression and allow IroC-mediated activation of Rh3 in **y**R7s in this region. *rh4>ss* generates a positive feedback loop to increase levels of Ss specifically in **y**R7s. These increased levels of Ss caused repression of Rh3 in **y**R7s in the DT (Figure 4A, 4G), showing that Ss must be maintained at low levels to allow for Rh3 expression.

Therefore, Rh3 and Rh4 appear to be differentially responsive to modulation of Ss levels in regions of the retina: Whereas Rh3 repression is sensitive to the reduction of Ss levels in the DT, Rh4 activation is robust. We characterized these differences further by evaluating a series of ss and *tgo* mutant alleles that cause premature termination and truncation of activation domains, leading to reduction in activity levels (Figure 2B, Figure 5A). To determine the molecular lesions, we sequenced the $ss^{116.4}$, tgo^{6} and other ss alleles (Figure 2B, Figure 5A, Materials and Methods). Including the ectopic expression of Ss experiment, we observed six phenotypic classes:

1. *Increased levels in **y**R7s (rh4>ss)*: Rh3 and Rh4 were expressed in stochastically distributed, complementary subsets of R7s throughout the retina, including the DT where Rh3 became excluded from **y**R7s (Figure 4A, 4G)
2. *Wild type (tgo^{3}):* Rh3 and Rh4 were expressed in stochastically distributed, mutually exclusive subsets of R7s in the majority of the retina (i.e. DE, VE, and VT). Rh3 was expressed in Rh4-expressing **y**R7s in the DT (Figure 4B, 4G).
3. *Weak loss-of-function (tgo^{6}, tgo^{1}):* De-repression of Rh3 occurred readily in yR7s of the DT and DE regions and sporadically in the VT and VE regions. Rh4 remained expressed in stochastically distributed **y**R7s (Figure 4C, 4G).
4. *Medium loss-of-function (tgo^{5}):* De-repression of Rh3 occurred in nearly all R7s. Rh4 was still expressed in stochastically distributed yR7s (Figure 4D, 4G).
5. *Strong loss-of-function ($ss^{d116.4}$/def, $ss^{d116.5}$/def):* De-repression of Rh3 occurred in nearly all R7s. Rh4 was still expressed in stochastically distributed **y**R7s, but the frequency was subtly reduced in the DT region (Figure 4E, 4G).
6. *Null ($ss^{d115.7}$, tgo^{del6}, tgo^{del25}):* Rh3 was expressed and Rh4 was lost in all R7s (Figure 4F–G)

These data show that Rh3 and Rh4 respond differently to Ss/Tgo activity levels. Lowering Ss/Tgo activity allowed for de-repression of Rh3 without affecting activation of Rh4 in yR7s. Rh3 was susceptible to an underlying dorsal/ventral gradient of regulation since the region in which Rh3 co-expresses with Rh4 in **y**R7s expanded ventrally as Ss/Tgo activity decreased. Whereas Rh3 was very sensitive to Ss/Tgo activity levels, Rh4 was robust, with only subtle changes in the frequency of Rh4 expression observed in the DT (where Ss levels are reduced) in the strongest loss-of-function alleles. Our data suggest that Ss/Tgo activity occurs at specific levels to induce repression of Rh3 in **y**R7s throughout the majority of the retina while allowing co-expression with Rh4 in **y**R7s of the DT region.

Rh regulation is sensitive to the activation capacity of Ss

The *ss/tgo* allelic series suggested that the C-terminal activation domains are important for the regulation of Rh expression in R7s. For the *tgo* alleles, the degree of activation domain truncation correlated with the loss of activation capacity and phenotypic severity (Figure 2B, Figure 4C–D, Figure 4F–G) (Sonnenfeld et al., 2005).

To further characterize the differential response of Rh3 and Rh4 to Ss/Tgo activity levels, we used gain of function assays with Ss proteins with deletions of functional domains. The

Ss bHLH domain binds DNA sequences in target genes upon dimerization with Tgo. The PAS domains mediate Ss/Tgo dimerization whereas the PAC motif contributes to folding of the PAS domain. The C-terminal region functions as an activation domain (Figure 5A) (Crews, 1998; Crews and Fan, 1999; Ponting and Aravind, 1997; Zhulin et al., 1997).

Considering our allelic series analysis, we predicted that Ss protein whose C-terminal activation domain had been truncated should activate Rh4 but not repress Rh3. We generated wild type and modified *UAS>Ss* ($Ss^{modified}$) constructs that lacked one or more of the distinct functional domains ($Ss^{\Delta AS/PAC}$ $Ss^{\Delta bHLH}$, $Ss^{\Delta PAS\text{-}N}$, $Ss^{\Delta PAS\text{-}C}$ $Ss^{\Delta PAC}$) or had truncations of the C-terminal activation region ($Ss^{\Delta C1}$, $Ss^{\Delta C2}$, $Ss^{\Delta C3}$) (Figure 5A–B). Upon ectopic $Ss^{modified}$ expression (*panR7>Gal4; UAS>*$Ss^{modified}$), we observed three classes of phenotypes that corroborated our *ss/tgo* allelic series:

1. $Ss^{wild\ type}$, $Ss^{\Delta PAS\text{-}C}$, $Ss^{\Delta PAC}$, *and* $Ss^{\Delta C1}$ *induced expression of Rh4 and repression of Rh3 in all R7s* (Figure 5B–C, Figure S2J–K, S20-Q), suggesting that these constructs were fully functional. It was surprising that the second PAS domain and the PAC domain were not required to regulate Rh expression since they have important roles for PAS-bHLH protein function.
2. $Ss^{\Delta C2}$ *and* $Ss^{\Delta C3}$ *induced Rh4 but did not repress Rh3 in* ***p****R7s* (Figure 5B, 5D, Figure S2J, S2R-S), consistent with the phenotype observed for ss and *tgo* mutants with truncated C-terminal domains.
3. $Ss^{\Delta bHLH}$, $Ss^{\Delta PAS\text{-}N}$, *and* $Ss^{\Delta PAS/PAC}$ *caused no change in Rh expression* (Figure 5B, 5E, Figure S2J, S2L-N), consistent with critical roles for the bHLH and N-terminal PAS domains. We confirmed that these non-functional transgenes were indeed expressed using Ss antibody staining (Figure S2E–I).

Truncation of the C-terminal region reduces the transcriptional activity of the Ss protein. However, these changes in Ss could also impair heterodimerization with Tgo, prevent nuclear localization, or destabilize the protein in a non-specific way. We therefore tested the $Ss^{modified}$ proteins for their capacity to localize Tgo to the nucleus. Ectopic expression of Ss driven by the *engrailed* promoter (*en>Gal4*) caused Tgo nuclear localization in the ectodermal *en* stripes in the fly embryo (Figure 5B, 5F) (Emmons et al., 1999). Another PAS-bHLH partner of Tgo, Trachealess, localizes Tgo to the nucleus in tracheal tubules and salivary primordia, serving as an internal control for Tgo antibody staining (Figure S2T–BB) (Ward et al., 1998).

$Ss^{\Delta C1}$, $Ss^{\Delta C2}$, $Ss^{\Delta C3}$ induced Tgo nuclear localization as well as $Ss^{wild\ type}$, suggesting that truncation of the C-terminal activation region does not impair heterodimerization, localization, or stability (Figure 5B, 5F, Figure S2T, S2Z–BB). $Ss^{\Delta PAC}$ was also sufficient to induce Tgo nuclear localization, consistent with the dispensability of the PAC domain in the retina (Figure 5B, 5F, Figure S2Y). Interestingly, $Ss^{\Delta PAS\text{-}C}$ was only able to induce lower levels of Tgo localization (Figure 5B, 5G, Figure S2X), suggesting that the C-terminal PAS domain increases the efficiency for dimerization and nuclear localization but is not absolutely required. As expected, $Ss^{\Delta bHLH}$, $Ss^{\Delta PAS\text{-}N}$, *and* $Ss^{\Delta PAS/PAC}$ were not able to induce Tgo nuclear localization (Figure 5B, 5H, Figure S2U–W).

This structure/function analysis of Ss is consistent with the *ss/tgo* allelic series. Ss and Tgo proteins with truncations of the C-terminal activation domains causing reduced activity levels were able to induce Rh4 expression, but not Rh3 repression.

Stochastic and regional expression of Rh3 is controlled by repressing and activating inputs

Ss/Tgo does not regulate *rh3* directly, but rather activates Dve to repress *rh3* in yR7s (Figure 1A–B). However, Dve is expressed at levels that allow IroC to overcome repression and activate Rh3 in **y**R7s of the DT region (Johnston et al., 2011). We wondered whether Dve expression levels were affected in hypomorphic mutant situations that displayed Rh3 de-repression. In tgo^5 mutant clones, Dve expression was decreased but not lost (Figure 6A–B). Thus, the dramatic changes in Rh3 expression observed upon modulation of Ss/Tgo activity appear to be mediated by changes in Dve levels.

rh3 regulation is controlled by repressing (Dve) and activating (Otd, Sal, IroC) inputs. We next tested whether the sensitivity of *rh3* regulation extends to its promoter. The *rh3* promoter contains three canonical binding sites **(TAATCC)** for the K_{50} homeodomain transcription factors, Dve and Otd (Figure 6C) (Johnston et al., 2011; Tahayato et al., 2003). In **y**R7s, these sites appear to mediate repression by Dve. A 194 bp *rh3* promoter (*rh3prom>GFP*) induced expression in only **p**R7s in the main part of the retina and in both **p**R7s and **y**R7s in the DT region, similar to the Rh3 protein (Figure 6E). Mutation (K_{50} *mut1*) of the distal K_{50} site (K_{50}–1) caused de-repression in **y**R7s of the DE region (Figure 6F) whereas mutation (K_{50} *mut2*) of the proximal site (K_{50}–2) led to de-repression in **y**R7s of the DE and VE regions (Figure 6G). Mutation of both sites (K_{50} *mut12*) caused de-repression in **y**R7s throughout the retina (Figure 6H).

We next tested the roles of the four putative IroC binding sites in the *rh3* promoter (Figure 6C)(Bilioni et al., 2005). Mutation of 3 of 4 sites (*IroC mut134*) or all 4 sites caused a complete loss of expression in DT **y**R7s (Figure 6D and data not shown). Both sets of mutations caused some loss of expression in **p**R7s, suggesting that these sites may also play a limited role in basal activation of *rh3*. These data suggest that IroC directly binds the *rh3* promoter to upregulate expression in the DT.

Thus, Dve and IroC binding sites are critical for the sensitivity of *rh3* to this regulatory network, dictating regional activation or repression outcomes in **y**R7s. The dorsal/ventral effects of these promoter mutations closely mirror the *ss/tgo* allelic series (Figure 4A–F, Figure 6D–H).

In summary, removing IroC activity or IroC binding sites causes loss of Rh3 expression in DT **y**R7s whereas ectopic expression of IroC at high levels induces Rh3 in the main region (Figure 6D)(Mazzoni et al., 2008). Removing Ss/Tgo or Dve activity, or Dve binding sites causes de-repression in the main region whereas increasing levels of Ss/Tgo or Dve causes repression of Rh3 in DT **y**R7s (Figure 4A–G, Figure 6A–B, Figure 6F–H)(Johnston et al., 2011). We conclude that Rh3 expression in DT **y**R7s is controlled by both activation by IroC and a release of repression by Dve (and indirectly Ss) on the *rh3* promoter.

Rh4 activation is robust to modulation of Ss/Tgo activity

The Ss/Tgo heterodimer is a transcriptional activator that could act directly on the *rh4* promoter to induce expression. Ss/Tgo binds Xenobiotic Response Elements (XREs; core sequence: **CACGC)** to activate target genes (Emmons et al., 1999). A 455 bp *rh4* promoter (*rh4prom>GFP*) induced expression that recapitulates endogenous Rh4 expression in **y**R7s (Figure 7A–B) (Fortini and Rubin, 1990). We identified one core XRE site that is conserved in all 12 sequenced *Drosophila* species examined (Figure 5D). The XRE is part of a larger element previously defined as RUS4A (TTTGCGGG**CACGC**AA) that is required for *rh4* reporter expression (Fortini and Rubin, 1990). A single point mutation in the XRE (to **CAAGC)** led to nearly complete abrogation of reporter expression (<2% R7s expressed

GFP)(Figure 7B–C). Thus, the XRE sequence is required for *rh4* expression, strongly suggesting that Ss/Tgo directly binds the *rh4* promoter to induce expression.

Since Ss levels were lower in the DT, we wondered if Rh4 transcription levels were also reduced. Rh4 protein appears to be lower in the DT, although this could be due to Rh4 competing with Rh3 protein for rhabdomeric space. We assessed *rh4* transcription with the *rh4prom>GFP* reporter gene, which showed no difference in levels between the DT (where Ss levels are low) and VT (where Ss levels are high)(Figure 7E–F), suggesting that reduction in Ss levels in the DT does not affect Rh4 expression. We also evaluated *rh4prom>GFP* in mutant clones that have reduced Ss/Tgo activity. *rh4prom>GFP* was expressed at similar levels in tgo^5 and neighboring wild type clones (Figure 7G–H), suggesting that activation of *rh4* is robust to perturbations of Ss/Tgo activity. Since Ss is expressed at lower levels in the DT, the responsiveness of the *rh4* promoter ensures that Rh4 is still activated there. In contrast, *rh3* expression is sensitive to levels of Ss/Tgo activity to induce expression in DT **y**R7s and repression in main region **y**R7s.

Discussion

The complex expression pattern of Rhs in R7s requires the integration of stochastic and regional regulatory information. In the main part of the retina, high levels of Ss in **y**R7s ensure repression of Rh3 and activation of Rh4. In the DT, reduced Ss levels allow IroC-mediated activation of Rh3, yet are sufficient to activate Rh4.

IroC activates Rh3 in the DT where Ss levels are lower (Figure 8H). In *IroC* mutants, even the low levels of Ss in the DT are sufficient to induce repression of Rh3 (indirectly through Dve) (Figure 8G). Reciprocally, high levels of IroC are sufficient to induce Rh3 in the main part of the retina despite the presence of normal levels of Ss (Figure 8I)

The regional regulation of *rh3* also requires reduction of Ss (and Dve) levels in the DT. In wild type animals, Ss levels are high in **y**R7s in the main region to induce repression of Rh3 and low in the DT to allow Rh3 expression (Figure 8B). Increasing the levels of Ss in the DT causes Rh3 repression in **y**R7s (Figure 8A). As the activity of Ss/Tgo is lowered in mutant conditions, Rh3 expression expands ventrally in the DE (Figure 8C) and then throughout the retina (Figure 8D–F). This intermediate expansion into the DE may be explained by the dynamic nature of IroC expression. IroC is initially expressed in all cells of the dorsal half (DT and DE) of the retina and then becomes restricted to the DT (Mazzoni et al., 2008; Sato and Tomlinson, 2007; Tomlinson, 2003). Perhaps, residual levels of IroC and/or chromatin changes induced at the *rh3* promoter increase the activation capacity of *rh3* in the DE (Figure 8B–C). At low levels of Ss activity or with complete ablation, the general activators Sal and Otd induce expression of Rh3 in all R7s, including those in the ventral half (VE and VT)(Figure 8D–F). These observations support the requirement for the modulation of Ss levels to ensure proper regional Rh3 regulation. The presence of multiple K_{50} (repressing via Dve and activating via Otd) and IroC (activating) binding sites in the *rh3* promoter is consistent with the nature of this regulatory mechanism.

In contrast, the control of Rh4 appears to be much simpler: Ss/Tgo, even at low levels, induces Rh4 expression (Figure 8B), likely by directly binding the lone canonical XRE (Ss/Tgo binding site) in the *rh4* promoter. Perturbations of Ss/Tgo that yield derepression of Rh3, do not affect Rh4 expression (Figure 8C–D). A subtle decrease in the frequency of Rh4 expression occurs in the DT where Ss levels are reduced only when Ss/Tgo activity is strongly impaired, likely because Ss/Tgo activity levels are near the threshold for activation (Figure 8E). Therefore, *rh4* is highly responsive to Ss ensuring that it is expressed in **y**R7s in the DT where Ss levels are low.

Ss expression is controlled by two main inputs: stochastic On/Off regulation and regional modulation of levels. The random, binary input determines **p**R7 (Ss Off) vs. **y**R7 (Ss On) fate whereas the regional input determines main region (Ss high) vs. DT (Ss low) **y**R7 fate. Though IroC is considered the critical factor determining dorsal identity in the retina, it does not appear to control regional modulation of Ss levels. Rather, another mechanism must work in parallel with IroC to control aspects of dorsal identity.

Despite dramatic changes in the activity of Ss and Tgo, Rh4 remains expressed in ~65% of R7s. If the mechanism controlling stochastic subtype specification was dependent on Ss levels (e.g. via a feedback mechanism), a decrease in Ss/Tgo activity levels should cause a decrease in the frequency of Rh4-expressing **y**R7s with a concomitant increase in the number of Rh3-expressing **p**R7s. Here, we have shown that this is not the case: Ss levels do not play a role in determining the frequency of stochastic expression but rather are modulated to allow Rh3 expression in Rh4-expressing **y**R7s in the DT. Thus, the stochastic mechanism controlling Ss expression requires regulation of the ss promoter independent of feedback.

Proper Rhodopsin expression requires tight regulation of the levels of stochastically-expressed Ss. If Ss levels were highly variable, we would expect to see de-repression of Rh3 in other R7s throughout the retina. Instead, we only observe expression of Rh3 in DT **y**R7s consistent with our findings that Ss levels are specifically lower there.

Our ongoing promoter dissection reveals that, not surprisingly, ss is controlled by a complex *cis*-regulatory logic (Johnston and Desplan, submitted). It will be interesting to see how the ss gene integrates these two dramatically different types of inputs to produce its complex expression pattern.

Experimental Procedures

Drosophila strains and crosses

Flies were raised on standard corn-meal-molasses-agar medium and grown at 25°C. Below, we list all shortened genotypes, complete genotypes, figures in which they are examined, and original source for each reagent:

Short Genotype	Complete Genotype	Figures	Source
wild type	*yw*; +; + or *yw*; *sp/CyO*; + *or yw*; *sp/CyO*; *TM2/TM6b*	1D–F, 2C, 2G, 3A–H	
ss null mutant	*ey>flp;+; FRT82b SS$^{d115.7}$ / FRT82b GMR>hid, cL*	2D, 2H, 4G	*ey>flp* (Newsome et al., 2000) *FRT82b GMR>hid* (Stowers and Schwarz, 1999) *FRT82b ss$^{d115.7}$* (Duncan et al., 1998)
tgo^{de16} null mutant	*ey>flp;+; FRT82b tgo^{de16}/ FRT82b GMR>hid, cL*	2A–B, 2E, 21, 4F–G	
tgo^{de125} null mutant	*ey>flp;+; FRT82b tgo^{de125} / FRT82b GMR>hid, cL*	2A–B, S1A, 4G	
tgo RNAi	*UAS>Dicer2; ey>Gal4, GMR>gal4/+; UAS>tgo RNAi/+*	2F	*UAS>Dicer2, ey>Gal4, GMR>gal4*, and *UAS>tgo RNAi* [VDRC stock center]
RNAi control	*UAS>Dicer2; ey>Gal4, GMR>gal4/+; +*	S1B	

Short Genotype	Complete Genotype	Figures	Source
tgo^{de16} mutant clones	*ey>flp;+; FRT82b tgo^{de16} / FRT82b ubi>GFP*	2J–L, S1C–G	*FRT82b ubi>GFP* [Bloomington stock center]
GMR>ss; tgo^{de16} mutant clones	*ey>flp; IGMR>Gal4, UAS>ss/ +; FRT82b tgo^{de16} / FRT82b ubi>GFP*	2M–N	*IGMR>Gal4* (Wernet et al., 2003) *UAS>ss* (Duncan et al., 1998)
tgo^{prom}>nuGFP	yw; +;*tgo^{prom}*>GFP /+	20	
wild type single cell clones	*hs>flp, elav>Gal4, UAS>mcd8GFP /+; +; FRT82b tubpGal80 / FRT82b +*	S1H, S1L	
ss single cell mutant clones	*hs>flp, elav>Gal4, UAS>mcd8GFP /+; +; FRT82b tubpGal80 / FRT82b ss$^{d115.7}$*	S1I.S1L	
tgo^{de16} single mutant clones	*hs>flp, elav>Gal4, UAS>mcd8GFP /+; +; FRT82b tubpGal80 /FRT82b tgo^{del6}*	S1J, S1L	
tgo^{de125} mutant clones	*hs>flp, elav>Gal4, UAS>mcd8GFP /+; +; FRT82b tubpGal80 / FRT82b tgo^{del25}*	S1K, S1L	
IroC mutant clones	*ey>flp;+; FRT80 Df(3L)iro^{DFM3} / FRT80ubi>GFP*	3I–J	
rh4>ss	*yw; rh4>Gal4 / UAS>ss^{modified}; +/+*	4A, 4G	
wild type whole eye clone	*ey>flp;+; FRT82b + / FRT82b GMR>hid, cL*	4B, 4G	
tgo^{3} mutant	*ey>flp;+; FRT82b tgo^{3} / FRT82b GMR>hid, cL*	4G	*FRT82b tgo^{3}* (Sonnenfeld et al., 1997; Sonnenfeld et al., 2005)
tgo^{6} mutant	*ey>flp;+; FRT82b tgo^{6} / FRT82b GMR>hid, cL*	4C, 4G	*FRT82b tgo^{6}* (Emmons et al., 1999)
tgo^{1} mutant	*ey>flp;+; FRT82b tgo^{1} / FRT82b GMR>hid, cL*	4G	*FRT82b tgo^{1}* (Sonnenfeld et al., 1997)
tgo^{5} mutant	*ey>flp;+; FRT82b tgo^{5} / FRT82b GMR>hid, cL*	4D, 4G	*FRT82b tgo^{5}* (Emmons et al., 1999; Tajiri et al., 2007)
ss$^{116.4}$ /def mutant	*yw; +;ss$^{116.4}$ / Df(3R)Exel7330*	4G	*ss$^{116.4}$* (Duncan et al., 1998) *Df(3R)Exel7330* [Bloomington stock center]
ss$^{116.5}$ /def mutant	*yw; +;ss$^{116.5}$ / Df(3R)Exel7330*	4E, 4G	*ss$^{116.5}$* (Duncan et al., 1998)
panR7>ss^{modified}; h4^{prom}>GFP, subsequently panR7>ss^{modified}	*yw; panR7>Gal 4/ UAS>ss^{modified}; rh4prom>GFP / +*	5B–E, S2A–D, S2J–S	
IGMR>ss^{modified}; rh4^{prom}>GFP, subsequently IGMR>ss^{modified}	*yw; IGMR>Gal4 / UAS>ss^{modified}; rh4prom>GFP / +*	S2A–I	
en>ss^{modified}	*yw; en>Gal4 / UAS>ss^{modified}; +*	5B,5F–H, S2T–BB	*en>Gal4* [Bloomington stock center]
tgo^{5} mutant clones	*ey>flp;+; FRT82b tgo^{5} / FRT82b ubi>GFP*	6A–B	
rh3$^{prom\ IroCmut134}$>GFP	prom IroCmut134	6D	

Short Genotype	Complete Genotype	Figures	Source
rh3$^{prom\ wild\ type}$*>GFP*	yw; +; *rh3*$^{prom\ wild\ type}$*>GFP*	6E	
rh3$^{prom\ K50\ mut1}$*>GFP*	yw; +; *rh3*$^{prom\ K50\ mut1}$*>GFP*	6F	
rh3$^{prom\ K50\ mut2}$*>GFP*	yw; *+*; *rh3*$^{prom\ K50\ mut2}$*>GFP*	6G	
rh3$^{prom\ K50\ mut12}$*>GFP*	yw; +; *rh3*$^{prom\ K50\ mut12}$*>GFP*	6H	
rh4^{prom}*>GFP*	yw; +; *rh4*^{prom}*>GFP / +*	7A–B, 7E–F	
rh4^{prom}*>GFP* (Point mutation)	yw; +; *rh4*^{prom}*>GFP / +*	7C	
tgo^{5} mutant clones; *rh4*^{prom}*>GFP*	*ey>flf; rh4*^{prom}*>GFP / +; FRT82b tgo*^{5} */ FRT82b +*	7G–H	

Note: For UAS>Ss^{modified} genotypes, these P-element transgenes were on either chromosome two or chromosome three. We list only chromosome two for simplicity.

Antibodies

Antibodies and dilutions used were as follows: mouse anti-Rh3 (1:10) (gift from S. Britt, University of Colorado), rabbit anti-Rh4 (1:100)(gift from C. Zuker, Columbia University), mouse anti-Rh5 (1:200) (Chou et al., 1996), rabbit anti-Rh6 (1:2000) (Mikeladze-Dvali et al., 2005; Tahayato et al., 2003), guinea pig anti-Ss 2.21 (1:200)(gift from Y.N. Jan, University of California, San Franscisco)(Kim et al., 2006), rabbit anti-Dve (1:500) (Nakagoshi et al., 1998), mouse anti-prospero (1:10)(DSHB), ms anti-Tgo (1:1, concentrated 10X)(DSHB), rat anti-ElaV (1:50) (DSHB), rabbit anti-Sens (1:100)(Xie et al., 2007), rat anti-Sal (1:100)(Barrio et al., 1999), guinea pig anti-Otd (1:750)(Vandendries et al., 1996), sheep anti-GFP(1:500) and Alexa488 Phalloidin (1:80) (Invitrogen). All secondary antibodies were Alexa-conjugated (1:400) (Molecular Probes).

Antibody staining (pupal and adult retinas)

Adult or staged pupal retinas were dissected and fixed for 15 minutes with 4% formaldehyde at room temperature. Retinas were rinsed two times in PBX and washed in PBX for >2 hours. Retinas were incubated with primary antibodies diluted in PBX overnight at room temperature and then rinsed two times in PBX and washed in PBX for >4 hours. Retinas were incubated with secondary antibodies diluted in PBX overnight at room temperature and then rinsed two times in PBX and washed in PBX for >2 hours. Retinas were mounted in Slofade (adult retinas) or Vectashield (pupal retinas). Images were acquired using an SP5 Leica confocal microscope (Hsiao et al., 2012; Rister et al., 2013).

Antibody staining (embryos)

Embryos were collected, dechorionated, fixed and devitellinated. Embryos were washed three times and then stored in methanol. For staining, methanol was removed and embryos were rinsed and washed in PBX. Embryos were incubated with primary antibodies overnight at 4C and then rinsed two times in PBX and washed in PBX for >4 hours. Embryos were incubated with secondary antibodies diluted in PBX overnight at 4C and then rinsed two times in PBX and washed in PBX for >4 hours. Embryos were mounted in Aquapolymount (Polysciences, Inc.) and images were acquired using an SP5 Leica confocal microscope.

Initial screening of UAS>Ss^{modified} lines with water immersion microscopy

We used the *panR7>Gal4* (expressed in all R7s) and *IGMR>Gal4* (expressed in all PRs) drivers to induce *UAS>Ss*^{modified} expression in the eye and examined *rh4*^{prom}>GFP expression. Flies were adhered to a Petri dish using nail polish and immersed in water. The retina was observed for GFP expression using a compound fluorescence microscope (40x

lens)(Pichaud and Desplan, 2001).We tested a minimum of two independent lines and found consistent results among lines (Figure S2A–D). We selected a single line for each UAS>Ss^{modified} transgene for further analysis.

Generating *tgo* null alleles

The *P(wHy)tgo^{DG08708}* transposable element in *tgo* was used to generate null mutant alleles (Huet et al., 2002). *yw*; +; *P(wHy)tgo^{DG08708} /TM3* flies were crossed with *yw; CyO, P(hsHT-2)/ ln(2LR)Gla, wg^{Gla-1}*; +. Parents were flipped after one day of egg laying. Progeny were heat shocked 30 minutes each day for four consecutive days. *yw; cyo,P(HSHT-2)/+; P(wHy)tgo^{DG08708} /+* progeny were crossed with *yw*; +; + and their progeny were screened for $w^{-}y^{+}$. $w^{-}y^{+}$ deletion stocks were established.

tgodelprimer1 (5’-GAAGCTACGACCATGGGAGG-3’) and *tgodelprimer2* (5’-ACGCAAAACACCGTATTGATTCGG-3’) were used to amplify the *tgo* locus and determine the size of the deletion. Amplicons were sequenced to precisely determine the deleted sequence.

Generating da neuron clones

For MARCM, *FRT* +, *FRTss^{d1157}, FRT82b tgo^{del6}* or *FRT82b tgo^{del25}* flies were mated to *elav-GAL4, UAS-mCD8::GFP, hs-FLP; FRT82 tubP-GAL80* flies (Lee and Luo, 2001). Embryos were collected for a 2 hr period and aged for 3 hr at 25°C. Embryos were then heat-shocked at 39°C for 50 minutes, allo wed to recover for 30 minutes at 25°C, then heat-shocked again at 39°C for 45 min. A nimals were reared at 18°C until the wandering larval stage, when GFP-positive clones were imaged. Morphology was analyzed in larval fillet preparations (Ye et al., 2004) immunostained with 1:350 Alexa Fluor 488 rabbit anti-GFP (Invitrogen), mounted in 70% glycerol, and imaged on a Leica SP5 confocal microscope using a 40x/1.25 NA oil objective. The total number of terminal branches was quantified in projections of individual ddaC neurons from the second through fifth abdominal segment as previously described (Lee et al., 2003). In Figure S1L, all error bars are ± one standard deviation around the mean.

Transgenes

tgo^{prom}>GFP—The *tgo* promoter was PCR amplified from wild type flies (*tgopromprimer1:* 5’-CTGCAGCATGTGCATGTGCTACGACTG-3’ and *tgopromprimer2:* 5’-GGATCCGCTTGGAATGCGTAATTAGAAAACG-3’) and cloned into the P-GEMT Easy vector. The *tgo* promoter was subcloned into an attB vector containing nuclearGFP using Pstl and BamHI. Constructs were inserted into the J36 attP site (gift of K. Basler) on the third chromosome using *phi-C31* mediated transgenesis (Bischof et al., 2007).

UAS>ss^{modified}—Fragments of ss were amplified from ss cDNA (Duncan et al., 1998), and subcloned into PCR-TOPOII vectors. Constructs were sequenced. ss fragments were subcloned into a modified pUAST vector (containing w^{+}) using EcoRI, Bglll, and Xbal. Constructs were injected into *yw* flies and independent transgenic (w^{+}) lines were established.

Below is the list of primers used to generate *UAS>ss^{modified}* constructs:

	Fragment 1	Fragment 2
Wild type	For:5'-GAATTCATGAGCCAGCTGGGCACCGTC-3' Rev:5'-TCTAGAGCGGTGGCCGTGGTGCAGGTG-3'	N/A
PAS/PAC del	For:5'-GAATTCATGAGCCAGCTGGGCACCGTC-3' Rev:5'-AGATCTCAGGCCGTGCTCGAAGGC-3'	For:5'-AGATCTGAGGGCCACGATCTGCTGGGC-3' Rev:5'-TCTAGAGCGGTGGCCGTGGTGCAGGTG-3'
bHLH del	For:5'-GAATTCATGAAGGATAAGGAGGATAACGGAGTC-3' Rev:5'-TCTAGAGCGGTGGCCGTGGTGCAGGTG-3'	N/A
PAS-N del	For:5'-GAATTCATGAGCCAGCTGGGCACCGTC-3' Rev:5'-AGATCTCAGGCCGTGCTCGAAGGC-3'	For:5'-AGATCTCTGCCCGCCGACATGTCC-3' Rev:5'-TCTAGAGCGGTGGCCGTGGTGCAGGTG-3'
PAS-C del	For:5'-GAATTCATGAGCCAGCTGGGCACCGTC-3' Rev:5'-AGATCTCGGCCCGAAGGGCGTGCAGTAGGC-3'	For:5'-AGATCTACGGGTGCCTCTGGCATGATC-3' Rev:5'-TCTAGAGCGGTGGCCGTGGTGCAGGTG-3'
PAC-del	For:5'-GAATTCATGAGCCAGCTGGGCACCGTC-3' Rev:5'-AGATCTGCCAGAGGCACCCGTCTTCAAAAG-3'	For:5'-AGATCTGAGGGCCACGATCTGCTGGGC-3' Rev:5'-TCTAGAGCGGTGGCCGTGGTGCAGGTG-3'
C-trun1	For:5'-GAATTCATGAGCCAGCTGGGCACCGTC-3' Rev:5'-TCTAGACTCGTCCATCAGCTGGCGGTG-3'	N/A
C-trun2	For:5'-GAATTCATGAGCCAGCTGGGCACCGTC-3' Rev:5'-TCTAGAAGCAGGGGATCCCACCTGGCC-3'	N/A
C-trun3	For:5'-GAATTCATGAGCCAGCTGGGCACCGTC-3' Rev:5'-TCTAGACGAGGAGCAAGATATCACCTC-3'	N/A

rh3^{prom}#x0003E;GFP—The *rh3* promoter was PCR amplified from yw flies and flanked by Bglll and Notl sites (*rh3promprimer1:* 5'-AGATCTGCACTAACCTTCAGATGAGC-3' and *rh3promprimer2:* 5'-GCGGCCGCGTCTGCGGGCCAAGACGAAATCA-3') and cloned into the pGEM-T Easy vector.

rh3$^{prom\ IroC134}$>GFP—IroC motifs 1 and 4 were mutated by amplifying the wild type promoter using modified oligos with mutations at the 5' and 3' end (*JR3FWIroc1mut* 5'-AGATCTGCACTAACCTTCAGATGAGCTGCACTTAGCC-3' and *JR3REVIroc4mut:* 5'-GCGGCCGCGTCTGCGGGCCAAGACGAAATCTAGGC-3'). The QuikChange mutagenesis kit (Stratagene) was used to mutate the IroC motif 3 (*JR3lroCmut3AFor:* 5'-GGTAATCCCGCTGCGTAGATGCTAATCCAATTC-3' and *JR3lroCmut3ARev:* 5'-GAATTGGATTAGCATCTACGCAGCGGGATTACC −3') to generate the *rh3^{promlroC134}>GFP* construct.

rh3$^{prom\ IroC1234}$>GFP—The QuikChange mutagenesis kit was used to mutate the IroC motif 2 in *rh3$^{prom\ lroC134}$>GFP (JR3lroCmut2HthAFor:* 5'-CAGTGCCAGCGAAAAATCCAGCAAGGGATTAGG −3' and *JR3lroCmut2HthARev:* 5'-CCTAATCCCTTGCTGGATTTTTCGCTGGCACTG −3') to generate the *rh3^{promlroC1234}>GFP*construct.

rh3$^{prom\ K5Omut1}$>GFP, rh3$^{prom\ K5Omut2}$>GFP, rh3$^{prom\ K5Omut12}$>GFP—The QuikChange mutagenesis kit was used to mutate the K_{50}−1 (*rh3mutprimer1For:* 5'-GCCAGCGAAAATGTCAGCAAGGGGCGAGGCCAATCCCAAACGGGTAATC-3'and *rh3mutprimer1Rev:* 5'-GATTACCCGTTTGGGATTGGCCTCGCCCCTTGCTGACATTTTCGCTGGC −3') and/or K_{50}−2 (*rh3mutprimer2For:* 5'-AGGCCAATCCCAAACGGGTCGCCCCGCTGCGACAATGCTA-3' and *rh3mutprimer2Rev:* 5'-TAGCATTGTCGCAGCGGGGCGACCCGTTTGGGATTGGCCT-3').

The *rh3* promoter and the mutated *rh3* promoters were subcloned into an attB vector containing GFP and miniwhite as selectable marker using Bglll and Notl. Constructs were inserted into the J36 attP site on the third chromosome using phi-C31 mediated transgenesis (Bischof et al., 2007).

***rh4^{prom}>GFP* and point mutation—**The *rh4* promoter was PCR amplified from transgenic flies (*rh4promprimer1:* 5'-CTTTGGAGTACGAAATGCGTC-3' and *rh4promprimer2:* 5'-GTCCAGCTCGACCAGGATGGG-3') and cloned into the P-GEMT Easy vector. The *rh4* promoter was subcloned into pBS using BamHI and EcoRI. *rh4mutprimerFor* (5'-CAATTAGACTTTGTGGTTGCTTGCCCGCAAAGACGATTTTC-3') and *rh4mutprimerRev* (5'-GAAAATCGTCTTTGCGGGCAAGCAACCACAAAGTCTAATTG-3') were used to induce the point mutation. The *rh4* promoter and the *rh4* promoter (point mutation) were subcloned into an attB vector containing GFP using BamHI and EcoRI. Constructs were inserted into the J36 attP site on the third chromosome using *phi-C31* mediated transgenesis (Bischof et al., 2007).

Quantification of expression

Using cell specific markers, antibody staining frequency was assessed for 5 or more retinas. >25 cells were scored per retina/region.

We used the LAS-AF software to quantified Ss levels in wild type animals (Figure 3A–H), Ss levels in **y**R7s ("On cells") in wild type and *IroC* mutant clones (Figure 3I–J), Dve levels in *tgo^{5}* mutants (Figure 6A–B), GFP levels in wild type DT and VT (Figure 7E–F), and GFP levels in wild type and *tgo^{5}* mutant clones (Figure 7G–H). A 1.3 urn in diameter circular "region of interest" was manually placed at the center of each R7 to avoid signal from neighboring PRs. LAS-AF software assessed the Pixel intensity for each region of interest for each R7.

All error bars in figures are ± one standard deviation around the mean.

Identification of molecular lesion in ss and *tgo* alleles

ss$^{d116.4}$—We PCR amplified and sequenced the coding regions of the ss gene. We identified a deletion causing missense mutations and early termination (Figure 5A).

tgo^{6}—We PCR amplified and sequenced the coding regions of the *tgo* gene. We identified a missense mutation causing early termination (Figure 2B).

Dp(3;2)P10—We used next-gen whole genome DNA sequencing to identify the breakpoint of this duplication in the ss locus (3R: 12,201,754).

T(1;3)ss^{D1143}—We used next-gen whole genome DNA sequencing to identify the breakpoints of this reciprocal translocation in the *ss* locus (3R: ~12,237,800) and X chromosome (Xhet: ~192,100).

SS^{GSG2553exc8o}—We generated imprecise P-element excision lines from the *P(Switch2)GSG2553* P-element. We used next-gen whole genome DNA sequencing to determine that this allele contains an inversion (breakpoint in *ss* at 3R: ~12,230,000) and a deletion (3R: ~12,230,000–12,235,000).

$ss^{RS6279exc44}$—We generated imprecise P-element excision lines from the *P(RS3)CB-6279–3* P-element. We used next-gen whole genome DNA sequencing to identify the endpoints of the deficiency that lie in the region upstream of the *ss* coding region (3R: 12,237,765) and in the second intron of the *Pak3* gene (3R: 12,274,176).

Supplementary Material

Refer to Web version on PubMed Central for supplementary material.

Acknowledgments

We are very grateful to S. Britt, S. Crews, I. Duncan, Y.N. Jan, C. Zuker, and the Bloomington Stock Center for reagents. E.C.O was supported by NIH F32 HD056779. We thank Cleopatra Tsanis and Terry Blackman for technical assistance. S.U.T., G.W.G, and A.Z. were supported by NYU Dean's Undergraduate Research Fund Grants. J.R. was supported by an EMBO long-term fellowship ALTF 462–2008. E.O.K. was supported by a NIH postdoc fellowship F32 HD056779. J.M.F. and M.D.P. were supported by the NYU Abu Dhabi Institute and the NSF Plant Genome Research Program. D.J. was supported by an NYU Dean's Dissertation Award. E.R.G. was supported by NIH R01 GM061107. CD. was supported by NIH R01 EY13010. R.J.J, was supported by a Jane Coffin Childs Memorial Fund for Medical Research postdoctoral fellowship.

References

Barrio R, de Celis JF, Bolshakov S, Kafatos FC. Identification of regulatory regions driving the expression of the Drosophila spalt complex at different developmental stages. Dev Biol. 1999; 215:33–47. [PubMed: 10525348]

Bell ML, Earl JB, Britt SG. Two types of Drosophila R7 photoreceptor cells are arranged randomly: a model for stochastic cell-fate determination. J Comp Neurol. 2007; 502:75–85. [PubMed: 17335038]

Bilioni A, Craig G, Hill C, McNeill H. Iroquois transcription factors recognize a unique motif to mediate transcriptional repression in vivo. Proc Natl Acad Sci U S A. 2005; 102:14671–14676. [PubMed: 16203991]

Bischof J, Maeda RK, Hediger M, Karch F, Basler K. An optimized transgenesis system for Drosophila using germ-line-specific phiC31 integrases. Proc Natl Acad Sci U S A. 2007; 104:3312–3317. [PubMed: 17360644]

Chou WH, Hall KJ, Wilson DB, Wideman CL, Townson SM, Chadwell LV, Britt SG. Identification of a novel Drosophila opsin reveals specific patterning of the R7 and R8 photoreceptor cells. Neuron. 1996; 17:1101–1115. [PubMed: 8982159]

Crews ST. Control of cell lineage-specific development and transcription by bHLH-PAS proteins. Genes Dev. 1998; 12:607–620. [PubMed: 9499397]

Crews ST, Fan CM. Remembrance of things PAS: regulation of development by bHLH-PAS proteins. Curr Opin Genet Dev. 1999; 9:580–587. [PubMed: 10508688]

Duncan DM, Burgess EA, Duncan I. Control of distal antennal identity and tarsal development in Drosophila by spineless-aristapedia, a homolog of the mammalian dioxin receptor. Genes Dev. 1998; 12:1290–1303. [PubMed: 9573046]

Emmons RB, Duncan D, Estes PA, Kiefel P, Mosher JT, Sonnenfeld M, Ward MP, Duncan I, Crews ST. The spineless-aristapedia and tango bHLH-PAS proteins interact to control antennal and tarsal development in Drosophila. Development. 1999; 126:3937–3945. [PubMed: 10433921]

Fortini ME, Rubin GM. Analysis of cis-acting requirements of the Rh3 and Rh4 genes reveals a bipartite organization to rhodopsin promoters in Drosophila melanogaster. Genes Dev. 1990; 4:444–463. [PubMed: 2140105]

Fujita PA, Rhead B, Zweig AS, Hinrichs AS, Karolchik D, Cline MS, Goldman M, Barber GP, Clawson H, Coelho A, et al. The UCSC Genome Browser database: update 2011. Nucleic Acids Res. 2011; 39:D876–D882. [PubMed: 20959295]

Hsiao HY, Johnston RJ Jr, Jukam D, Vasiliauskas D, Desplan C, Rister J. Dissection and immunohistochemistry of larval, pupal and adult Drosophila retinas. Journal of visualized experiments : JoVE. 2012

Huet F, Lu JT, Myrick KV, Baugh LR, Crosby MA, Gelbart WM. A deletion-generator compound element allows deletion saturation analysis for genomewide phenotypic annotation. Proc Natl Acad Sci U S A. 2002; 99:9948–9953. [PubMed: 12096187]

Johnston RJ Jr, Desplan C. Stochastic Mechanisms of Cell Fate Specification that Yield Random or Robust Outcomes. Annu Rev Cell Dev Biol. 2010

Johnston RJ Jr, Otake Y, Sood P, Vogt N, Behnia R, Vasiliauskas D, McDonald E, Xie B, Koenig S, Wolf R, et al. Interlocked feedforward loops control cell-type-specific rhodopsin expression in the Drosophila eye. Cell. 2011; 145:956–968. [PubMed: 21663797]

Kent WJ. BLAT-the BLAST-like alignment tool. Genome Res. 2002; 12:656–664. [PubMed: 11932250]

Kent WJ, Sugnet CW, Furey TS, Roskin KM, Pringle TH, Zahler AM, Haussler D. The human genome browser at UCSC. Genome Res. 2002; 12:996–1006. [PubMed: 12045153]

Kim MD, Jan LY, Jan YN. The bHLH-PAS protein Spineless is necessary for the diversification of dendrite morphology of Drosophila dendritic arborization neurons. Genes Dev. 2006; 20:2806–2819. [PubMed: 17015425]

Lee A, Li W, Xu K, Bogert BA, Su K, Gao FB. Control of dendritic development by the Drosophila fragile X-related gene involves the small GTPase Racl. Development. 2003; 130:5543–5552. [PubMed: 14530299]

Lee T, Luo L. Mosaic analysis with a repressible cell marker (MARCM) for Drosophila neural development. Trends Neurosci. 2001; 24:251–254. [PubMed: 11311363]

Mazzoni EO, Celik A, Wernet MF, Vasiliauskas D, Johnston RJ, Cook TA, Pichaud F, Desplan C. Iroquois complex genes induce co-expression of rhodopsins in Drosophila. PLoS Biol. 2008; 6:e97. [PubMed: 18433293]

Mikeladze-Dvali T, Wernet MF, Pistillo D, Mazzoni EO, Teleman AA, Chen YW, Cohen S, Desplan C. The growth regulators warts/lats and melted interact in a bistable loop to specify opposite fates in Drosophila R8 photoreceptors. Cell. 2005; 122:775–787. [PubMed: 16143107]

Nakagoshi H, Hoshi M, Nabeshima Y, Matsuzaki F. A novel homeobox gene mediates the Dpp signal to establish functional specificity within target cells. Genes Dev. 1998; 12:2724–2734. [PubMed: 9732270]

Newsome TP, Asling B, Dickson BJ. Analysis of Drosophila photoreceptor axon guidance in eye-specific mosaics. Development. 2000; 127:851–860. [PubMed: 10648243]

Pichaud F, Desplan C. A new visualization approach for identifying mutations that affect differentiation and organization of the Drosophila ommatidia. Development. 2001; 128:815–826. [PubMed: 11222137]

Ponting CP, Aravind L. PAS: a multifunctional domain family comes to light. Curr Biol. 1997; 7:R674–R677. [PubMed: 9382818]

Rister J, Desplan C, Vasiliauskas D. Establishing and maintaining gene expression patterns: insights from sensory receptor patterning. Development. 2013; 140:493–503. [PubMed: 23293281]

Sato A, Tomlinson A. Dorsal-ventral midline signaling in the developing Drosophila eye. Development. 2007; 134:659–667. [PubMed: 17215299]

Sonnenfeld M, Ward M, Nystrom G, Mosher J, Stahl S, Crews S. The Drosophila tango gene encodes a bHLH-PAS protein that is orthologous to mammalian Arnt and controls CNS midline and tracheal development. Development. 1997; 124:4571–4582. [PubMed: 9409674]

Sonnenfeld MJ, Delvecchio C, Sun X. Analysis of the transcriptional activation domain of the Drosophila tango bHLH-PAS transcription factor. Dev Genes Evol. 2005; 215:221–229. [PubMed: 15818484]

Sood P, Johnston RJ Jr, Kussell E. Stochastic De-repression of Rhodopsins in Single Photoreceptors of the Fly Retina. PLoS Comput Biol. 2012; 8:el002357.

Stowers RS, Schwarz TL. A genetic method for generating Drosophila eyes composed exclusively of mitotic clones of a single genotype. Genetics. 1999; 152:1631–1639. [PubMed: 10430588]

Tahayato A, Sonneville R, Pichaud F, Wernet MF, Papatsenko D, Beaufils P, Cook T, Desplan C. Otd/Crx, a dual regulator for the specification of ommatidia subtypes in the Drosophila retina. Dev Cell. 2003; 5:391–402. [PubMed: 12967559]

Tajiri R, Tsuji T, Ueda R, Saigo K, Kojima T. Fate determination of Drosophila leg distal regions by trachealess and tango through repression and stimulation, respectively, of Bar homeobox gene expression in the future pretarsus and tarsus. Dev Biol. 2007; 303:461–473. [PubMed: 17187773]

Tomlinson A. Patterning the peripheral retina of the fly: decoding a gradient. Dev Cell. 2003; 5:799–809. [PubMed: 14602079]

Vandendries ER, Johnson D, Reinke R. orthodenticle is required for photoreceptor cell development in the Drosophila eye. Dev Biol. 1996; 173:243–255. [PubMed: 8575625]

Ward MP, Mosher JT, Crews ST. Regulation of bHLH-PAS protein subcellular localization during Drosophila embryogenesis. Development. 1998; 125:1599–1608. [PubMed: 9521898]

Wernet MF, Labhart T, Baumann F, Mazzoni EO, Pichaud F, Desplan C. Homothorax switches function of Drosophila photoreceptors from color to polarized light sensors. Cell. 2003; 115:267–279. [PubMed: 14636555]

Wernet MF, Mazzoni EO, Celik A, Duncan DM, Duncan I, Desplan C. Stochastic spineless expression creates the retinal mosaic for colour vision. Nature. 2006; 440:174–180. [PubMed: 16525464]

Xie B, Charlton-Perkins M, McDonald E, Gebelein B, Cook T. Senseless functions as a molecular switch for color photoreceptor differentiation in Drosophila. Development. 2007; 134:4243–4253. [PubMed: 17978002]

Ye B, Petritsch C, Clark IE, Gavis ER, Jan LY, Jan YN. Nanos and Pumilio are essential for dendrite morphogenesis in Drosophila peripheral neurons. Curr Biol. 2004; 14:314–321. [PubMed: 14972682]

Zhulin LB, Taylor BL, Dixon R. PAS domain S-boxes in Archaea, Bacteria and sensors for oxygen and redox. Trends Biochem Sci. 1997; 22:331–333. [PubMed: 9301332]

Highlights

- Spineless (Ss) requires its dimeric partner Tango to control Rhodopsin expression
- Ss is expressed in a stochastic On/Off pattern throughout the retina
- In the main region, Ss at high levels ensures exclusive Rhodopsin expression
- In the dorsal third region, Ss at low levels allows for Rhodopsin co-expression

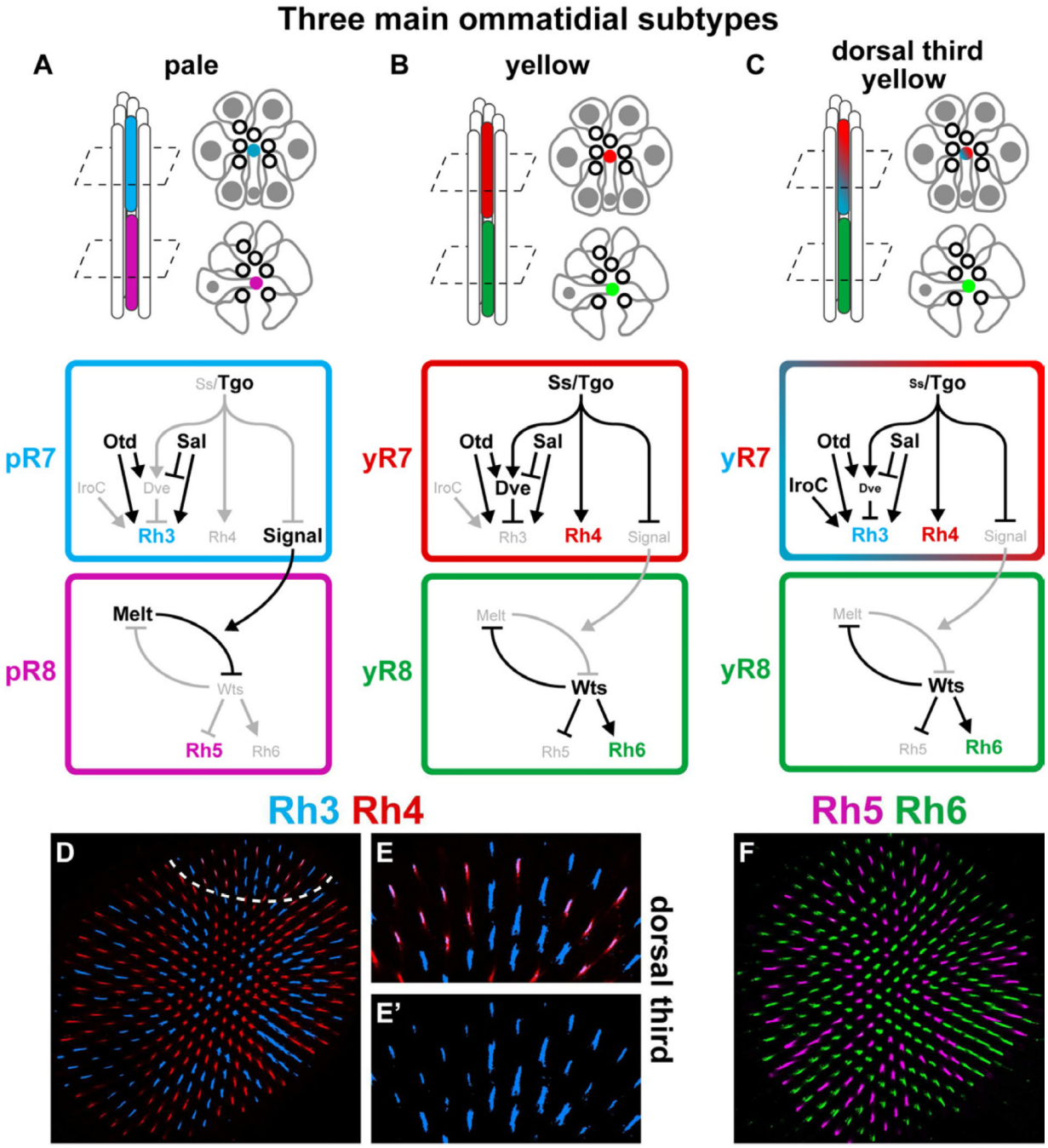

Figure 1. Rhodopsin expression in the fly eye

For A-C, top left indicates rhabdomeres (membranous structures containing Rh proteins) within an ommatidium. Top right indicates cross-sections in the R7 (top) and R8 (bottom) layers. Gray indicates cell bodies and nuclei. White circles with black outlines indicate outer PR rhabdomeres. Central, colored rhabdomeres indicate R7 (top) or R8 (bottom). Below, the regulatory network controlling Rh expression in R7 (top) or R8 (bottom).

A. **pale:** Rh3 (blue) is expressed in **p**R7s and Rh5 (purple) is expressed in **p**R8s. In the absence of Ss in **p**R7s, Sal represses Dve and acts with Otd to induce Rh3 expression. Rh4 expression is not activated. In the absence of Ss, a signal is de-

repressed which upregulates expression of the growth regulator Melted (Melt) in R8s. Melt represses the tumor suppressor Warts (Wts) inducing expression of Rh5 and repression of Rh6.

B. **yellow:** Rh4 (red) is expressed in **y**R7s and Rh6 (green) is expressed in **y**R8s. In **y**R7s, Ss activates Rh4 and Dve, which represses Rh3. Ss also represses the signal to R8. Melt is not expressed in the absence of the signal, allowing for Wts expression inducing expression of Rh6 and repression of Rh5.

C. **dorsal third yellow:** Rh3 (blue) and Rh4 (red) are expressed in **y**R7s and Rh6 (green) is expressed in **y**R8s. In **y**R7s, Ss activates Rh4 and Dve. In the dorsal third region, Ss levels are reduced to allow for IroC-mediated activation of Rh3. Ss also represses the signal to R8. Melt is not expressed in the absence of the signal, allowing for Wts expression inducing expression of Rh6 and repression of Rh5.

For D-F, dorsal is up and ventral is down.

D. In the main part of the retina, Rh3 and Rh4 are expressed in stochastic and exclusive subsets of R7s. Main part = below white dashed line; dorsal third region = above the white dashed line.

E. Higher magnification view of dorsal third region. In the dorsal third region, Rh3 is expressed in all R7s including Rh4-expressing yR7s. Top (Rh3 and Rh4) and bottom (Rh3 alone).

F. Rh5 and Rh6 are expressed in stochastic and exclusive subsets of R8s.

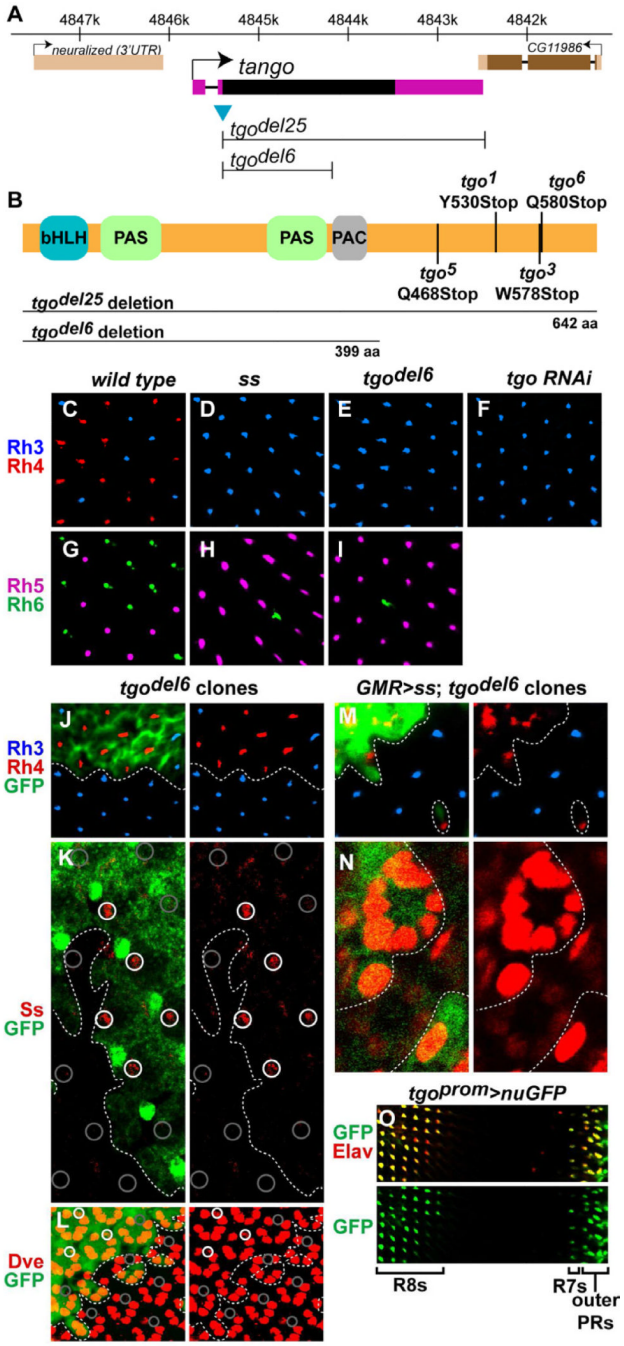

Figure 2. Tgo is required for Ss-mediated regulation of Rhs

A. Schematic of the *tgo* gene locus. The blue triangle indicates the P-element containing the hobo transposon used to generate the tgo^{del25} and tgo^{del6}molecular null alleles.

B. Schematic of the Tgo protein with mutant allele annotation.

C. Rh3 and Rh4 are expressed in random subsets of R7s in wild type animals.

D. Rh3 is expressed in all R7s in *ss* null mutants.

E. Rh3 is expressed in all R7s in *tgo*^{del6} null mutants.

F. Rh3 is expressed in all R7s when *tgo* is knocked down by RNAi.

G. Rh5 and Rh6 are expressed in random subsets of R8s in wild type animals.

H. Rh5 frequency increases (Rh6 decreases) in *ss* null mutants.

I. Rh5 frequency increases (Rh6 decreases) in *tgo*^{del6} null mutants.

For J-N, GFP- indicates *tgo*^{del6} mutant tissue; GFP+ indicates wild type tissue. Left, stain including GFP; Right, stain without GFP.

J. Rh3 is expressed in all R7s in *tgo*^{del6} clones. Rh3 and Rh4 are expressed in random subsets of R7s in wild type tissue.

K. Ss nuclear expression is lost in *tgo*^{del6} clones. Ss is expressed in random subsets of R7s in wild type tissue. White circles indicate Ss+ R7s; gray circles indicate Ss- R7s.

L. Dve expression is lost only in R7s in *tgo*^{del6} clones. Dve is expressed in random subsets of R7s in wild type tissue. Dve expression occurs in outer PRs in *tgo*^{del6}and wild type tissue. White circles indicate Dve+ R7s; gray circles indicate Dve-R7s.

M. Ectopic expression of Ss induces Rh4 in R7s and outer PRs in wild type tissue. Rh3 is expressed in all R7s in *tgo*^{del6} clones with ectopic expression of Ss.

N. Strong nuclear expression of Ss is observed upon ectopic expression in all PRs in wild type tissue. Weak nuclear expression of Ss is observed upon ectopic expression in all PRs in *tgo*^{del6} clones.

O. *tgo*^{prom}*>GFP* is expressed in all PRs of the retina including all R7s, R8s, and outer PRs. See also Figure S1.

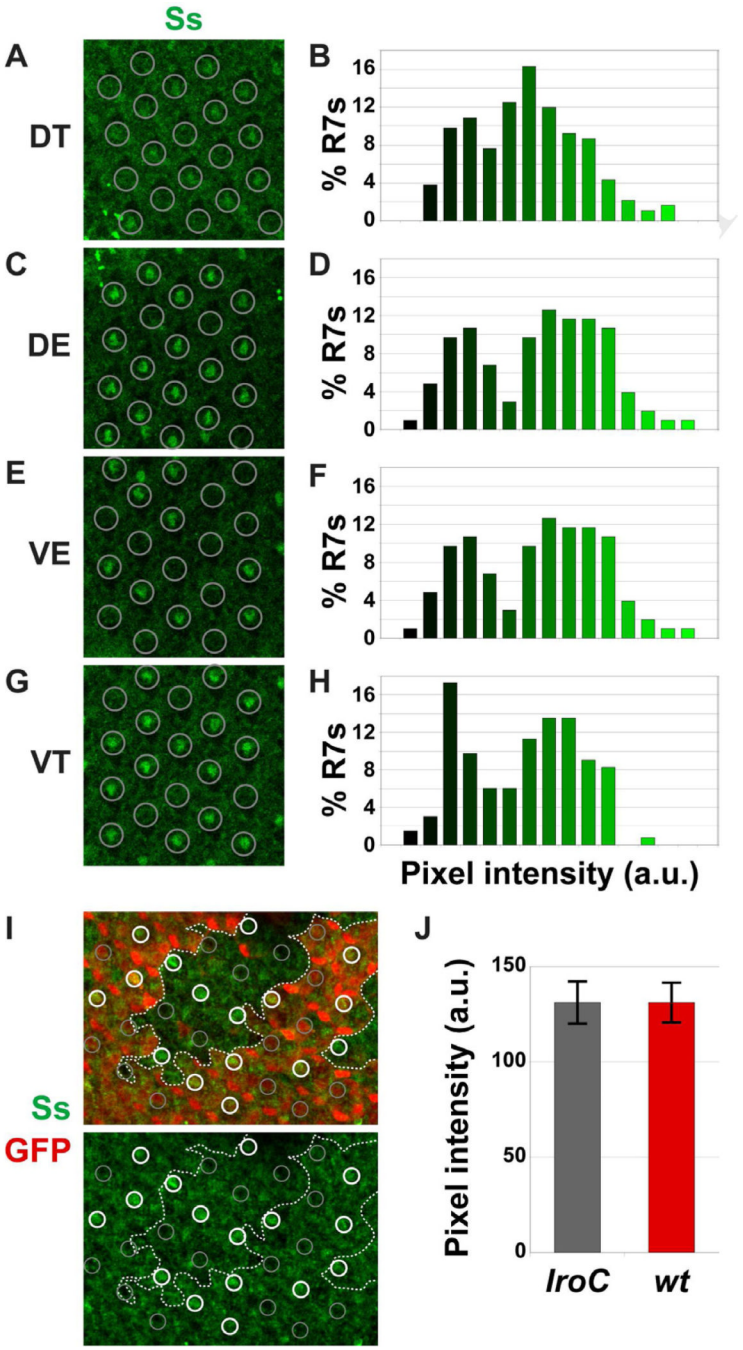

Figure 3. Ss levels are regionally modulated

For A-H, DT=dorsal third, DE=dorsal equatorial, VE=ventral equatorial, VT=ventral third. For B, D, F, and H, the bimodal distribution indicates the On/Off nature of Ss expression. The shift for the DT R7s (Figure 3B) shows the reduced levels of Ss expression in the On State in this region

A. Ss expression is lower in DT R7s.

B. Quantification of Ss expression in DT R7s.

C. Ss expression in DE R7s.

D. Quantification of Ss expression in DE R7s.

E. Ss expression in VE R7s.

F. Quantification of Ss expression in VE R7s.

G. Ss expression in VT R7s.

H. Quantification of Ss expression in VT R7s.

I. Ss levels are similar in *IroC* mutant and wild type clones. GFP- indicates *IroC* mutant tissue; GFP+ indicates wild type tissue. Top, Ss and GFP; Bottom, Ss alone. White circles indicate high Ss expression in **y**R7s; gray circles indicate no Ss expression in **p**R7s.

J. Quantification of Ss levels in *IroC* mutant and wild type clones. *IroC* mutant **y**R7s (gray) express Ss at similar levels to wild type **y**R7s (red).

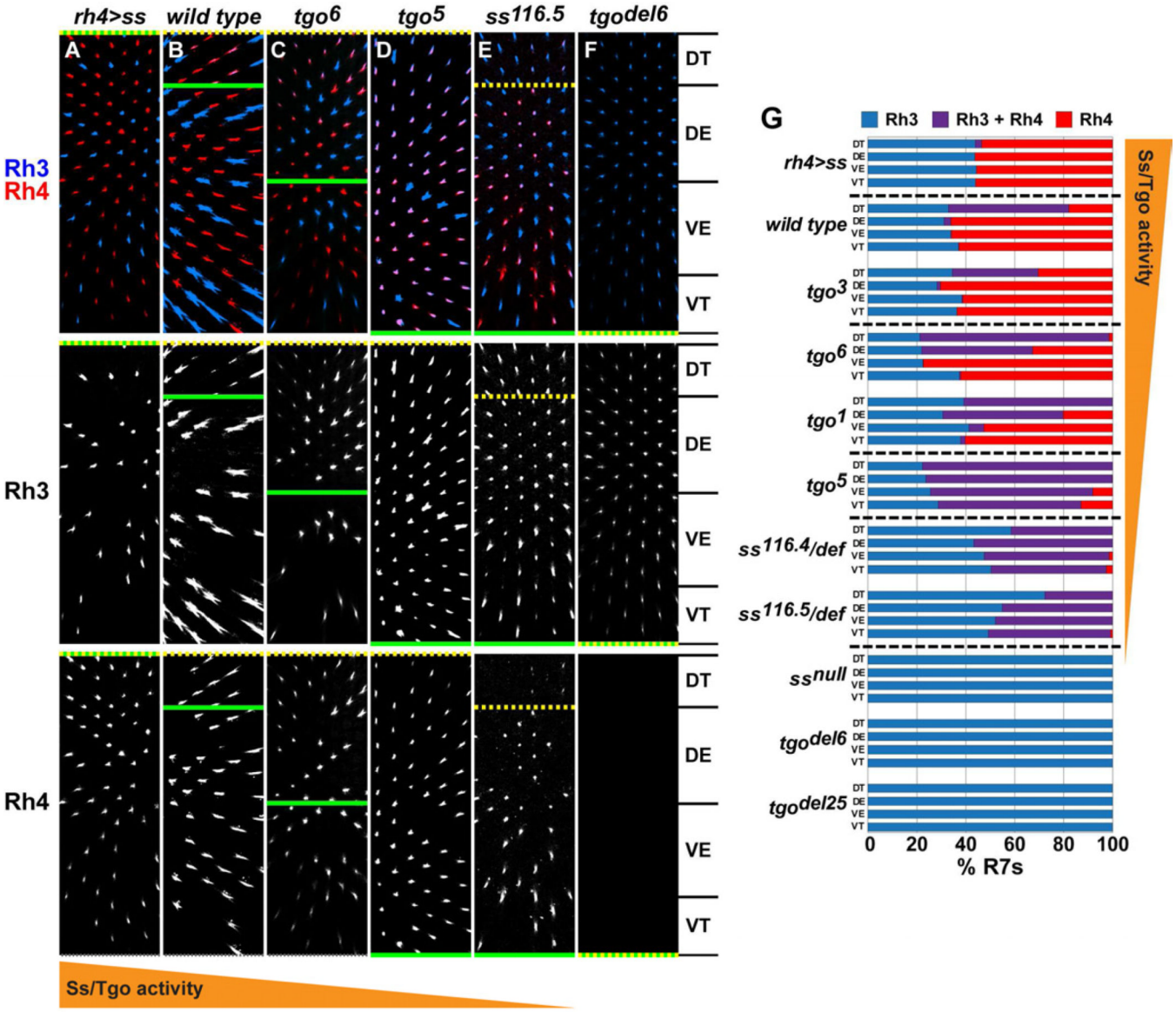

Figure 4. Rh3 and Rh4 are differentially responsive to Ss/Tgo activity levels

For A-G, DT=dorsal third, DE=dorsal equatorial, VE=ventral equatorial, VT=ventral third. For A-F, top, Rh3 and Rh4; middle, Rh3 alone; bottom, Rh4 alone. Green lines mark the regional boundary of Rh3 expression in **y**R7s. Dotted yellow lines mark the regional boundary of the normal frequency of Rh4 expression in **y**R7s.

- **A.** Ectopic expression of Ss (*rh4>ss*) represses Rh3 in dorsal third **y**R7s. Rh3 and Rh4 are expressed in exclusive subsets of R7s in all regions.
- **B.** In wild type animals, Rh3 and Rh4 are expressed in exclusive subsets of R7s in the DE, VE, and VT regions. The DT region is composed of R7s that express Rh3 alone or co-express Rh3 with Rh4.
- **C.** In *tgo*^{6} mutants, Rh3 expression in yR7s expands to the DE region. Rh3 and Rh4 are expressed in exclusive subsets of R7s in the VE and VT regions. The DT and DE regions are composed of R7s that express Rh3 alone or co-express Rh3 with Rh4.

D. In *tgo*^{5} mutants, Rh3 expression in **y**R7s expands to the entire retina. These retinas are composed of R7s that express Rh3 alone or co-express Rh3 with Rh4.

E. In *ss*^{1165} mutants, Rh3 expression in **y**R7s expands to the entire retina. These retinas are composed of R7s that express Rh3 alone or co-express Rh3 with Rh4. The frequency of Rh4 expression is slightly reduced in the DT.

F. In *tgo*^{del6} mutants, Rh4 is lost and Rh3 is expressed in all R7s throughout the retina.

G. Quantification of the series of *ss* and *tgo* alleles. Data is presented in order of decreasing Ss/Tgo activity (i.e. increasing phenotypic severity). The six main phenotypic classes are separated by dashed lines.

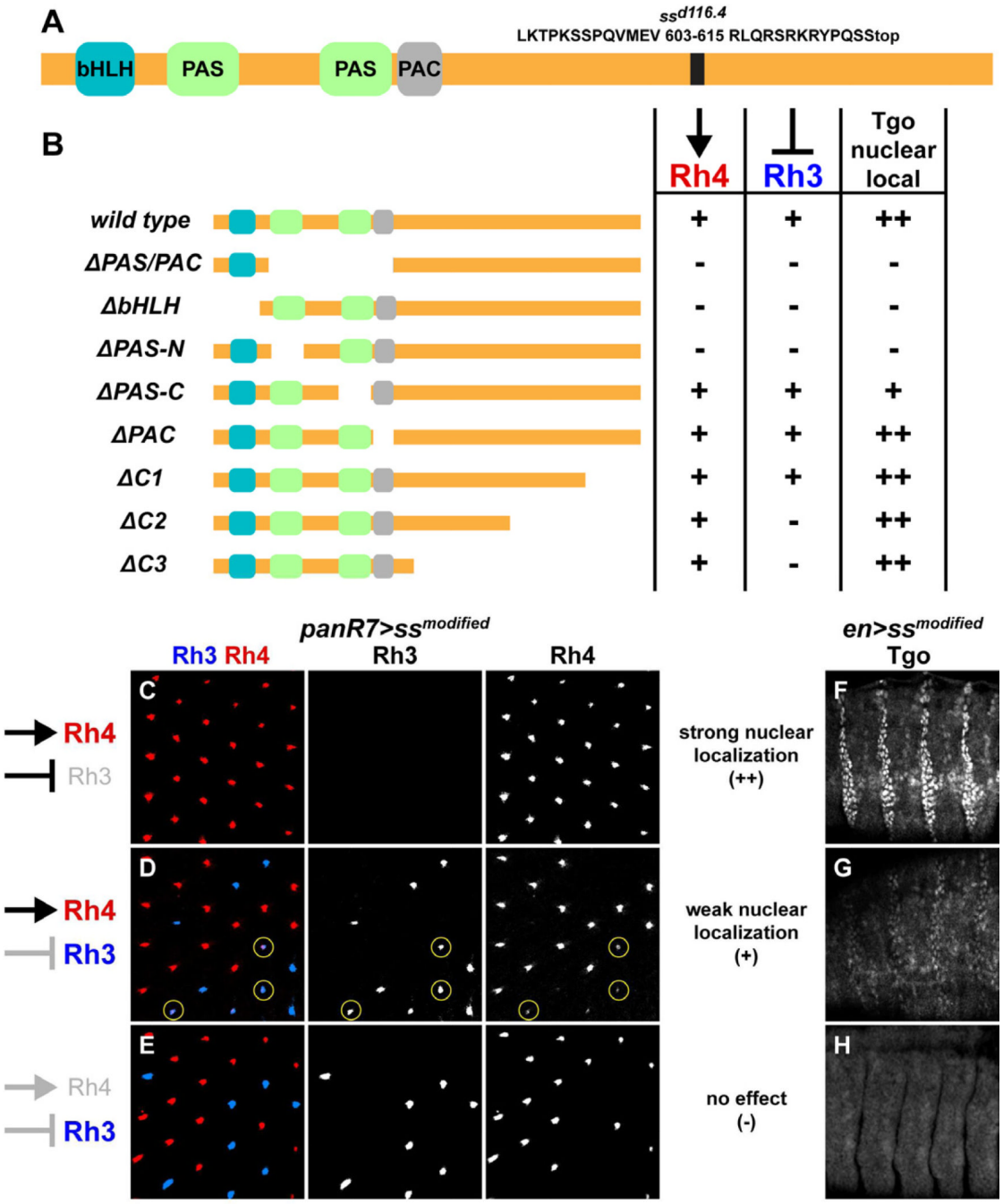

Figure 5. Ss/Tgo with reduced activity can activate Rh4 but not repress Rh3

A. Schematic of the Ss protein. The premature stop causing protein truncation in the *ss*$^{d116.4}$ allele is annotated.

B. Table summarizing Ss protein domain analysis. −> Rh4 = Rh4 activation; −| Rh3 = Rh3 repression; Tgo nuclear local = Tgo localization. (−) indicates no effect. (+) indicates an effect. For the Tgo nuclear localization assay, (++) indicates strong nuclear localization whereas (+) indicates weak nuclear localization.

For C-H, examples of each type of phenotype are shown. For Rh3/Rh4 expression and Tgo nuclear localization, image data for all constructs are shown in Figures S2K–BB. For C-E, examples of effects on Rh3/Rh4 expression. Left, Rh3 and Rh4 expression; middle, Rh3 alone; right, Rh4 alone. Expression was assessed in the main part of the retina (excluding the dorsal third).

C. Activation of Rh4 with repression of Rh3.

D. Activation of Rh4 without repression of Rh3. Yellow circles indicate examples of R7s that co-express Rh3 and Rh4.

E. No effect

F. For F-H, examples of effects on Tgo nuclear localization.

F. Strong nuclear localization of Tgo.

G. Weak nuclear localization of Tgo.

H. No effect.

See also Figure S2.

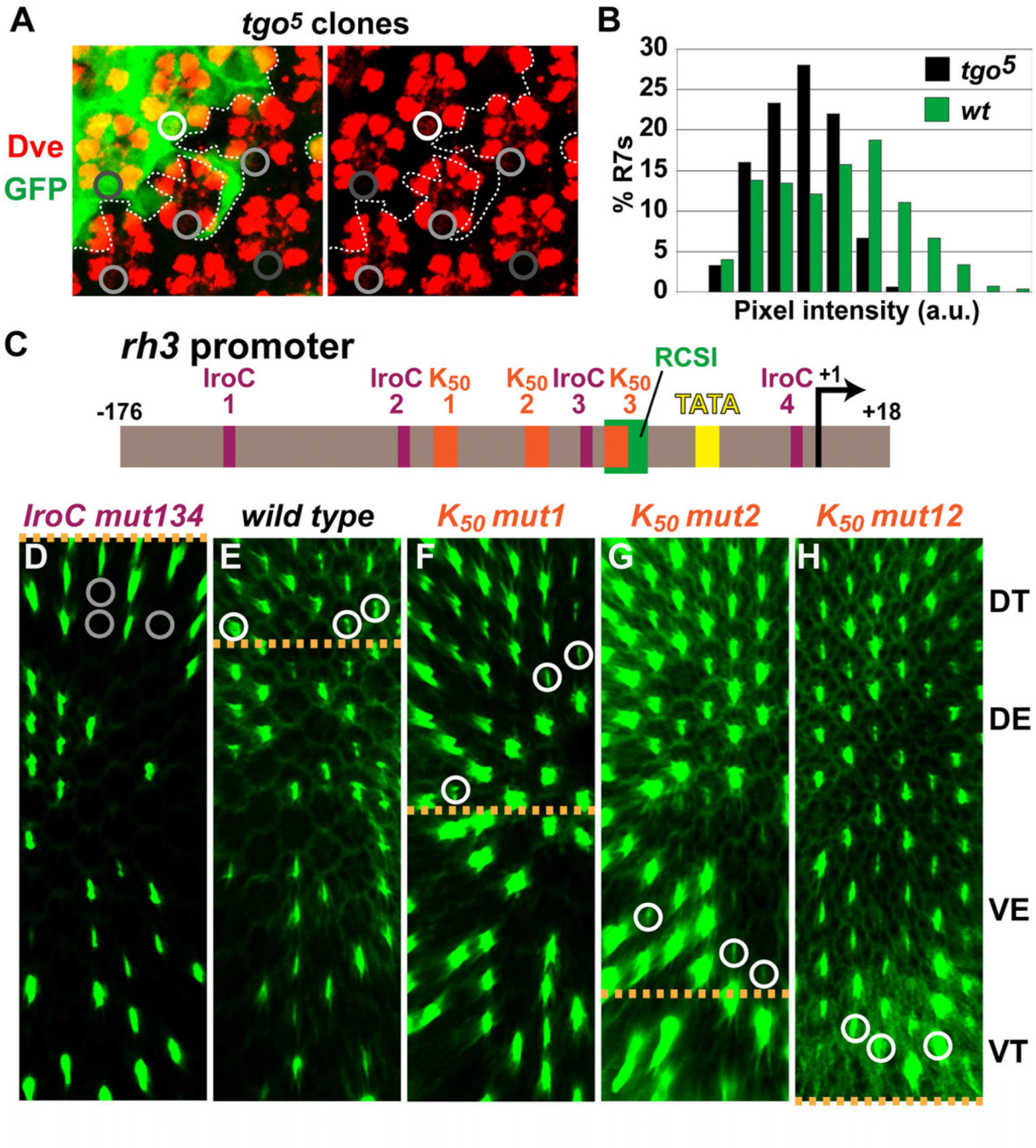

Figure 6. Regional *rh3* expression is sensitive to activating and repressing inputs

A. Dve levels in yR7s are decreased in *tgo*^{5} mutant clones. GFP- indicates *tgo*^{5}mutant tissue; GFP+ indicates wild type tissue. Left, Dve and GFP; Right, Dve alone. White circles indicate high Dve expression in wild type **y**R7s; light gray circles indicate low Dve expression in *tgo*^{5} mutant **y**R7s; dark gray circles indicate no Dve expression in wild type and *tgo*^{5} mutant **p**R7s

B. Quantification of Dve levels in *tgo*^{5} mutant clones and wild type tissue. Wild type R7s (green) express Dve at higher levels than *tgo*^{5} mutant R7s (black).

C. Schematic of *rh3* promoter that recapitulates Rh3 protein expression. Orange = K_{50}, Purple = *IroC* site, Green = *RCSI*, Yellow = *TATA* box. The RCSI is a conserved element found in all *rh* promoters that is required for expression.

For D, gray circles indicate DT yR7s that have lost expression of $rh3^{prom}>GFP$. For E-H, white circles indicate the ventral-most **y**R7s that express $rh3^{prom}>GFP$. For D-H, when *IroC* sites are mutated, expression of $rh3^{prom}>GFP$ is lost in DT **y**R7s, similar to the loss of expression observed when Ss levels are ectopically high. As K_{50} sites are mutated, de-repression of $rh3^{prom}>GFP$ expands ventrally similar to derepression of Rh3 protein in *ss/tgo* hypomorphic alleles. For all, $rh3^{prom}>GFP$ is expressed in **p**R7s in all regions of the retina. DT=dorsal third, DE=dorsal equatorial, VE=ventral equatorial, VT=ventral third. Dashed yellow lines mark regions where $rh3^{prom}>GFP$ is expressed in **y**R7s.

D. $rh3^{prom\ IroC\ mut134}>GFP$ is expressed in **p**R7s only. Expression in DT **y**R7s is lost.

E. $rh3^{prom\ wild\ type}>GFP$ is expressed in **y**R7s in the DT.

F. $rh3^{prom\ K50\ mut1}>GFP$ is expressed in **y**R7s in the DT and DE.

G. $rh3^{prom\ K50\ mut2}>GFP$ is expressed in **y**R7s in the DT, DE, and VE.

H. $rh3^{prom\ K50\ mut12}>GFP$ is expressed in **y**R7s throughout the retina (including DT, DE, VE, and VT).

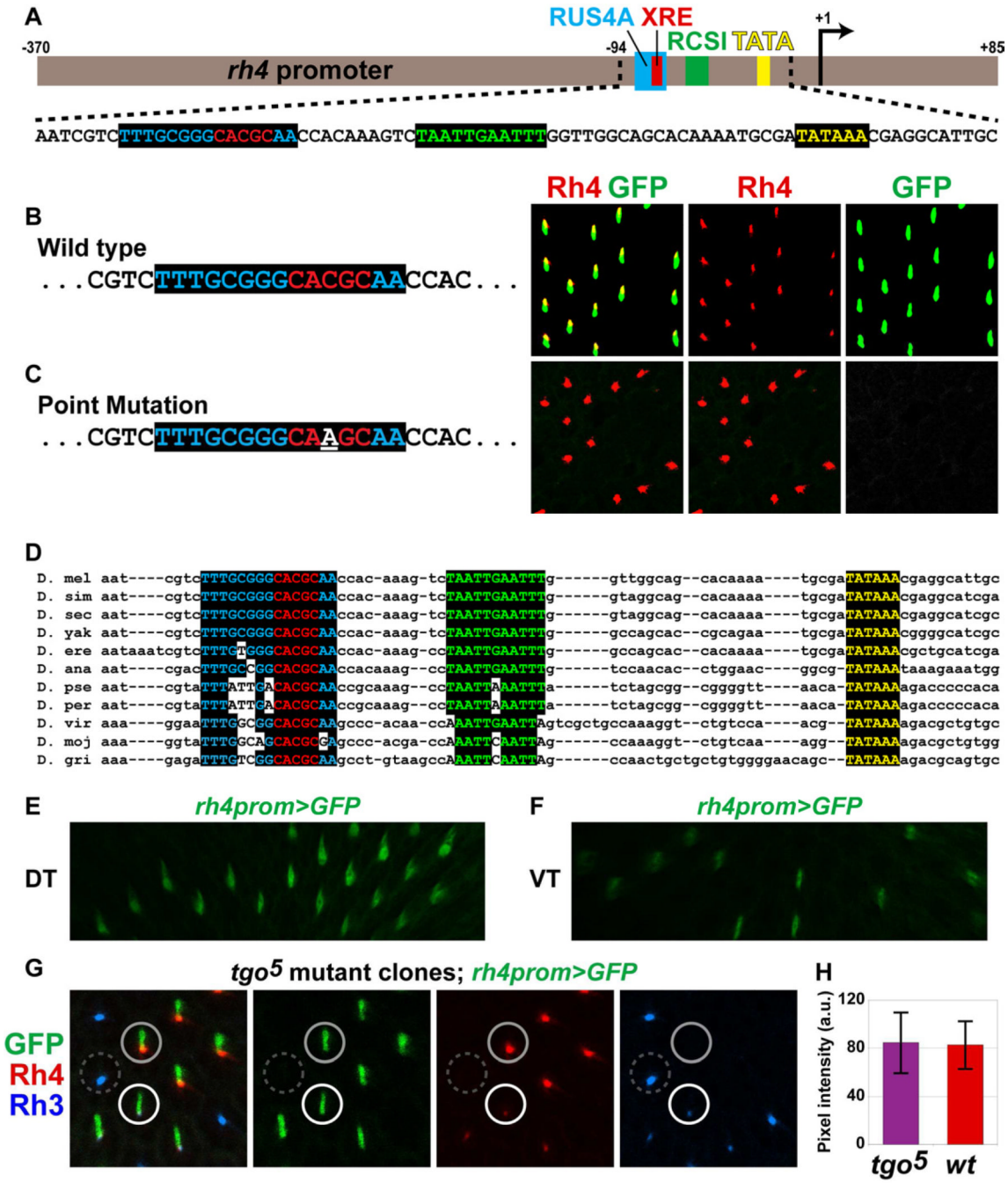

Figure 7. Robust Rh4 activation requires a canonical Ss binding site

For A-D, colors indicate known *cis*-regulatory regions. Blue = *RUS4A*, Red subset of *RUS4A* = XRE core site (Ss/Tgo binding site), Green = *RCSI* (inverted in *D. vir, D. moj, D. gri*), Yellow = *TATA* box.

- **A.** Schematic of *rh4* promoter that recapitulates Rh4 protein expression. Sequence shows known critical *cis*-regulatory elements.
- **B.** *rh4*^{prom}*>GFP* with wild type XRE recapitulates Rh4 protein expression.
- **C.** Expression is lost with a point mutation in the XRE.

D. Sequence alignment of the *rh4* promoter for 12 *Drosophila* species highlighting the known *cis*-regulatory elements. The XRE core sequence is perfectly conserved in all 12 species. Sequence alignment was from the UCSC Genome Browser (http://genome.ucsc.edu/) (Fujita et al., 2011; Kent, 2002; Kent et al., 2002).

E. $rh4^{prom}>GFP$ is expressed at similar levels in the DT.

F. $rh4^{prom}>GFP$ is expressed at similar levels in the VT.

G. $rh4^{prom}>GFP$ is expressed at similar levels in tgo^{5} and wild type **y**R7s. Panel 1: GFP, Rh4, and Rh3; Panel 2: GFP alone; Panel 3: Rh4 alone and Panel 4: Rh3 alone. The white circle indicates a tgo^{5} mutant yR7 that expresses $rh4^{prom}>GFP$ with both Rh3 and Rh4. The solid gray circle indicates a wild type **y**R7 that expresses $rh4^{prom}>GFP$ with Rh4 alone. The dotted gray circle indicates a pR7 that expresses Rh3 alone.

H. Quantification of $rh4^{prom}>GFP$ levels in tgo^{5} and wild type yR7s. tgo^{5} mutant **y**R7s (magenta) express $rh4^{prom}>GFP$ at similar levels to wild type **y**R7s (red).

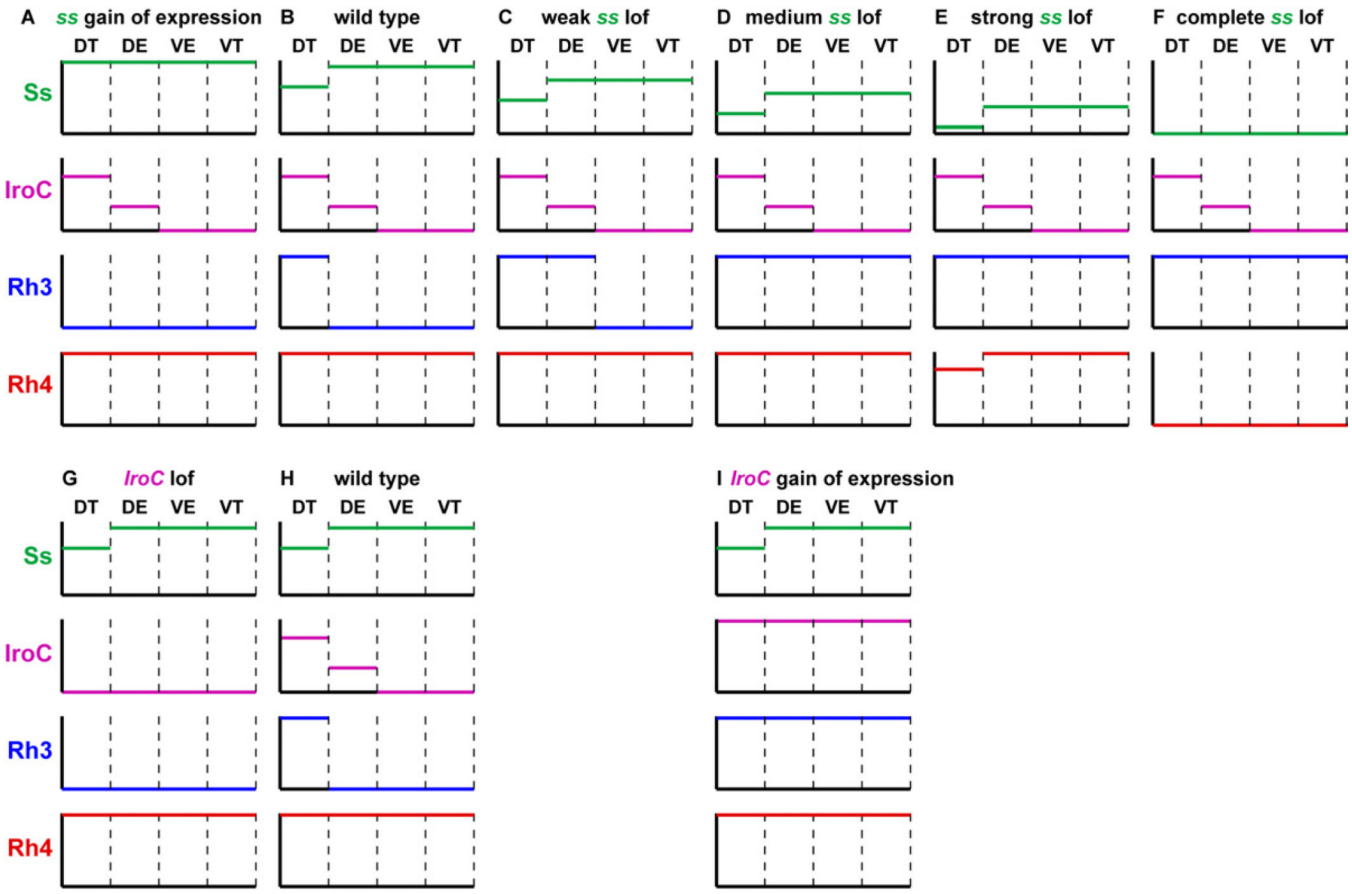

Figure 8. Model of region-specific regulation of Rh3 and Rh4 in yR7s by Ss and IroC

Green indicates Ss/Tgo activity levels; magenta indicates IroC activity levels; blue indicate Rh3 expression frequency in **y**R7s; and Red indicates Rh4 expression frequency in **y**R7s. As Ss/Tgo activity decreases (C–F) or IroC activity increases (I), Rh3 expression expands in **y**R7s. As Ss/Tgo activity increases (A) or IroC activity decreases (G), Rh3 expression is lost in **y**R7s. Despite changes in Ss/Tgo or IroC activity, the frequency of Rh4 expression is robust (A-D, G-l) with only subtle changes observed in the DT where Ss levels are low in strong *ss* lof (E).

lof = loss-of-function.

DT=dorsal third, DE=dorsal equatorial, VE=ventral equatorial, VT=ventral third.